Biochimica et Biophysica Acta, 553 (1979) 107—131

BBA 78346

POTASSIUM-STIMULATED ATPase ACTIVITY AND HYDROGEN TRANSPORT IN GASTRIC MICROSOMAL VESICLES *

HON-CHEUNG LEE, HAIM BREITBART, MARCIA BERMAN and JOHN G. FORTE

Department of Physiology-Anatomy, University of California, Berkeley, CA (U.S.A.)

(Received June 8th, 1978)
(Revised manuscript received October 16th, 1978)

Key words: K^+-ATPase; H^+/K^+ pump; Proton transport; Anion permeability; (Gastric microsome)

Summary

The Mg^{2+}-dependent, K^+-stimulated ATPase of microsomes from pig gastric mucosa has been studied in relation to observed active H^+ transport into vesicular space. Uptake of fluorescent dyes (acridine orange and 9-aminoacridine) was used to monitor the generated pH gradient. Freeze-fracture electron microscopy showed that the vesicular gastric microsomes have an asymmetric distribution of intramembraneous particles (P-face was particulate; E-face was relatively smooth).

Valinomycin stimulated both dye uptake and K^+-ATPase (valinomycin-stimulated K^+-ATPase); stimulation by valinomycin was due to increased K^+ entry to some intravesicular activating site, which in turn depends upon the accompanying anion. Using the valinomycin-stimulated K^+-ATPase and H^+ accumulation as an index, the sequence for anion permeation was $NO_3^- > Br^- > Cl^- > I^- >$ acetate $\approx$ isethionate. When permeability to both K^+ and H^+ was increased (e.g using valinomycin plus a protonophore or nigericin), stimulation of K^+-ATPase was much less dependent on the anion and the observed dissipation of the vesicular pH gradient was consistent with an 'uncoupling' of ATP hydrolysis from H^+ accumulation.

Thiocyanate interacts with valinomycin inhibiting the typical action of the K^+ ionophore. But stimulation of ATPase activity was seen by adding 10 mM SCN^- to membranes preincubated with valinomycin. From the relative activation of the valinomycin-stimulated K^+-ATPase, it appears that SCN^- is a very

* This work was presented in preliminary form in (1978) Fed. Proc. 37, 651 and (1978) Biophys. J. 21, 133a.

Abbreviations: Pipes, piperazine-*N*,*N*′-bis(2-ethane sulfonic acid); MalNEt, *N*-ethyl maleimide; DTNB, 5,5′-dithiobis-2-nitrobenzoic acid; Hepes, 4-(2-hydroxyethyl)-1-piperazineethane sulfonic acid; TCS, 3,3′,4′,5-tetrachloro salicylanilide; CCCP, carbonylcyanide-*m*-chlorophenyl hydrazone.

permeant anion which can be placed before NO_3^- in the sequence of permeation.

Valinomycin-stimulated ATPase and H^+ uptake showed similar dependent correlations, including: dependence on [ATP] and [K^+], pH optima, temperature activation, and selective inhibition by SH- or NH_2-group reagents.

These results are consistent with a pump-leak model for the gastric microsomal K^+-ATPase which was simulated using Nernst-Planck conditions for passive pathways and simple kinetics for the pump. The pump is a K^+/H^+ exchange pump requiring K^+ at an internal site. Rate of K^+ entry would depend on permeability to K^+ as well as the counterion, either (1) the anion to accompany K^+ or (2) the H^+ efflux path as an exchange ion. The former leads to net accumulation of H^+ and anion, while the latter results in non-productive stimulation of ATP hydrolysis.

Introduction

A preparation of microsomes isolated from fundic gastric mucosa of several species has been shown to possess Mg^{2+}-dependent, K^+-stimulated ATPase activity [1]. Immunocytochemical and other studies have demonstrated that these membranes are largely derived from oxyntic cells [2,3]. Furthermore, the gastric microsomal membranes can be isolated largely in a vesicular form and can transport (accumulate) H^+ in the presence of K^+, Mg^{2+} and ATP [2,4—6]. The principal conclusion from these former studies is that the gastric microsomal vesicles are characterized by an ATP-driven H^+/K^+ exchange transport.

Cations have obviously been linked to gastric vesicular transport; however, it would be of interest to assess the role of anions in the system as it might apply to secretory function of the intact tissue. The Cl^- requirements for H^+ secretion by gastric mucosa is well-known [7—9]. Relatively permeable anions (Br^-, Cl^-, I^-) support H^+ secretion [9], whereas impermeable ones, such as SO_4^{2-} or isethionate (2-hydroxyethylsulfonate), drastically curtail secretion [7,8]. It is also clear that Cl^- secretion by gastric mucosa is stimulated when H^+ transport is stimulated and inhibited when H^+ secretion is similarly reduced [10,11]. Such correlations between H^+ and Cl^- secretion have suggested some functional commonalities in the transport process, but it has not been possible to unequivocally distinguish between a direct biochemical coupling or indirect electrical coupling.

Early attempts to study the effects of anions on enzymatic reactions in isolated gastric membranes reported a HCO_3^--stimulated, SCN^--inhibited ATPase activity [12,13], but this system does not appear to be a fruitful one to pursue at the present time [3]. We have taken several established features of the gastric microsomal vesicles [1—6,14] to develop a working model for vesicular transport which incorporates a role for anions, and might be used for further testing. The relatively simple scheme depicted in Fig. 1 incorporates an ATP-driven transport of H^+ via some H^+/K^+ exchange mechanism. Ionophores or other experimental manipulations would operate to alter the passive fluxes of various ions and thus indirectly affect the ATPase and transport properties. Consistent with this scheme, we have shown that accumulation of H^+ depends upon the

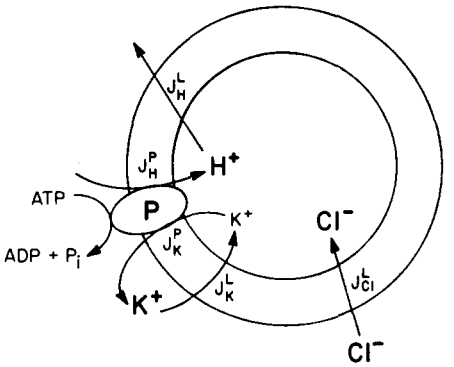

Fig. 1. Hypothetical scheme accounting for ion movements across gastric microsomal vesicles. The J values are the ionic fluxes with the superscripts designating pump flux (P) or leak pathway (L). The model consists of an ATP-driven H^+/K^+ exchange pump, in accord with earlier work (e.g. Refs. 4—6 and 14), and the passive leak pathways for the principal ions, K^+, H^+ and Cl^-.

presence of internal K^+, either by preincubating the vesicles in KCl solutions or by using valinomycin as an entry path for K^+ from the external solutions [14]. Addition of protonophores or K^+/H^+ exchangers (e.g. nigericin) lead to rapid dissipation of the proton gradient as would be qualitatively predicted from the scheme [2,5,6,14].

In this report, we will use fluorescent probes (acridine orange and 9-aminoacridine) to monitor H^+ transport in gastric membrane vesicles [14,15] and correlate the transport activity with that of K^+-ATPase activity. Our results demonstrate a coupling between H^+ gradient formation and ATPase activity. We will show that anions exert an effect on both the K^+-ATPase and H^+ transport activities by their limitation on the accessibility of K^+ to an internal pump site via the membrane potential. By the use of a series of activators and inhibitors, we will further substantiate this hypothesis of an internal K^+ site as the pump site. A computer simulation model of the ion transport properties of these gastric vesicles will also be presented.

Materials and Methods

Isolation of gastric microsomes. Gastric microsomes were isolated from hog stomach homogenates using differential centrifugation and further subfractionated using a discontinuous sucrose density gradient as described previously [16]. The lightest membrane band corresponding to density between 1.08 and 1.11 was used in this study.

Freeze-fracture microscopy. Gastric microsomes taken directly from the sucrose gradient were fixed lightly with 0.6% glutaraldehyde for 10 min at room temperature (21—24° C). Fixation was terminated by 3 fold dilution with cold homogenizing medium containing 113 mM mannitol, 37 mM sucrose, 0.2 mM EDTA and 5 mM piperazine-*N*,*N*′-bis(2-ethanesulfonic acid) (Pipes) buffer at pH 6.68. The fixed microsomes were harvested by centrifugation at 200 000 × g for 20 min at 5° C. The pellet was washed briefly and then

infiltrated with 20% glycerol for 5 h in the cold. Small pieces of the pellet were placed on cardboard discs, frozen in liquid freon 22 and fractured at −155°C under a high vacuum of $2 \cdot 10^{-6}$ Torr in a Balzers BA 360 M freeze-etch unit. Replicas were made by shadowing the fractured surface with platinum and carbon. The rest of the pellet was dissolved away by commercial sodium hypochlorite (Purex). The replica was washed twice with distilled water and mounted on naked 300-mesh copper grids and examined using the JEM 100C electron microscope operated at 100 kV.

ATPase measurements. ATPase activity was measured at room temperature (except where specified otherwise) by the liberation of inorganic phosphate in 1 ml of incubation medium containing 1 mM $MgSO_4$, 1 mM ATP, 20—30 μg membrane protein and 10 mM Pipes buffer at the designated pH. Other experimental additions are indicated for the individual experiments. The reaction was terminated with 1 ml of 14% CCl_3COOH. All of the enzyme determinations were carried out in duplicate; experiments were repeated in more than one preparation (usually several) of microsomal membranes. Inorganic phosphate was ordinarily determined by extraction of the phosphomolybdate complex into butyl acetate according to the method of Sanui [17]. This method was not satisfactory when SCN^- was used; for these latter experiments, the procedure of Eibl and Lands [18] was used to assay inorganic phosphate.

H^+ uptake. Vesicular acidification was measured by the accumulation of the fluorescent amines, 9-aminoacridine and acridine orange, as previously described [14]. In particular, it was shown that 9-aminoacridine distributes across the membrane as a weak base in accordance with the H^+ gradient and thus is a quantitative probe for the H^+ gradient. On the other hand, acridine orange showed characteristics of binding to membrane sites in addition to accumulation in response to the H^+ gradient. Because of the binding, the effect of the H^+ gradient on the uptake of acridine orange is magnified, and thus can serve as a highly sensitive, although qualitative, H^+ gradient probe.

The method uses the change in fluorescence intensity (quenching) which is proportional to the amount of dye taken up by the microsomes. All fluorescence measurements were made with the Perkin-Elmer MPF-44A spectrofluorimeter. Wavelengths used were 493 → 530 nm (excitation → emission wavelength) for acridine orange and 422 → 455 nm for 9-aminoacridine.

Sulfhydryl group modification. (1) *N*-Ethyl maleimide (MalNEt). Gastric microsomes (approx. 1 mg protein/ml) in 20% sucrose solution were reacted with 10 mM MalNEt for various periods of time. The reaction was terminated by 40—60-fold dilution and subsequently used for both dye uptake and ATPase assays.

(2) 5,5′-Dithiobis-2-nitrobenzoic acid (DTNB). The time course of the DTNB reaction was followed spectrophotometrically using the Aminco-Bowman dual wavelength instrument. The sample wavelength was set at 412 nm and the reference wavelength at 500 nm. Small aliquots of 10 mM DTNB were added to the cuvette containing about 0.4 mg/ml gastric microsomes in various media (as specified in individual experiments) to achieve a final DTNB concentration of 0.4 mM. Under conditions of excess reagent, the reaction of DTNB with sulfhydryl groups gives stoichiometric change in absorbance at 412 nm [19]; thus the kinetics of change can be used to measure the accessibility of differ-

ent microsomal SH groups to DTNB [20,21]. Semi-logarithmic plots of the absorbance data vs. time were graphically analyzed for distinguishable classes of sulfhydryl groups. The slope of each linear component represents the reaction rate of a class of SH groups, and the extrapolated absorbance at zero time is proportional to the number of groups in that class which can be calculated using an extinction coefficient of 13 600 at 412 nm [19].

The ATPase activity of the DTNB-treated membrane was assayed by stopping the DTNB reaction with addition of 0.8 mM cysteine at a designated time and aliquots were subsequently taken for the assay.

Amine group modification. The amino groups of the microsomes were modified by imidoester; both the monofunctional ethylacetimidate and bifunctional dimethylsuberimidate were used. Solid reagents were weighed out in containers, dissolved in 0.25 M sucrose with 50 mM 4-(2-hydroxyethyl)-2-piperazineethanesulfonic acid (Hepes), and NaOH was added to bring the pH to 8.5. Microsomes (1 mg/ml) were added to start the amidination. The final concentrations of the imidoester reagents were 20 mM and 10 mM for ethylacetimidate and dimethylsuberimidate, respectively. At a designated time, aliquots of reacted microsomes were taken out and the amidination reaction terminated by 10 fold dilution into 100 mM cold Tris buffer (Tris(hydroxymethyl)aminomethane) at pH 7.5. These reacted microsomes were then assayed for both ATPase activity and acridine orange uptake. The extent of the amidination was monitored by measuring the total remaining free amino groups on the reacted microsomes. This was done fluorimetrically using fluorescamine [22].

Miscellaneous. Protein content of various membrane fractions were measured according to the method of Lowry and coworkers [23]. Valinomycin, obtained from Sigma, was used as a K^+ ionophore. Ionophores for H^+ included 3,3,4′,5-tetrachlorosalicylanilide (TCS) from Eastman Kodak and carbonylcyanide-*m*-chlorophenyl hydrazone (CCCP) obtained from Sigma. The K^+/H^+ exchange ionophore, nigericin, was a gift from Dr. W.E. Scott, Hoffman La Roche Inc.

Results

Electron microscopic observations

Fig. 2 shows the freeze-fracture electronmicrograph of a pellet of the gastric membranes. It can be seen that this membrane fraction is composed of relatively homogeneous vesicular structures with sizes ranging from 1000—2000 Å in diameter. Two images of vesicular surfaces can be seen. Vesicles which cleaved convexly generally appeared smooth, although a few smooth concave vesicles were also seen. Vesicles which cleaved concavely were typically particulate in appearance. The particles were about 60—90 Å in diameter. The cleavage produced by freeze-fracturing occurs within the hydrophobic interior and parallel to the plane of the membrane [24]. The exposed faces of gastric vesicles are therefore related to the outer half (convex) and to the inner half (concave) of the membrane. The asymmetrical distribution of particles between the two membrane halves indicates that the particles have a stronger interaction with the outer half, as compared to the inner half of the membrane. Similar asymmetrical distribution of particles have also been observed in sarcoplasmic

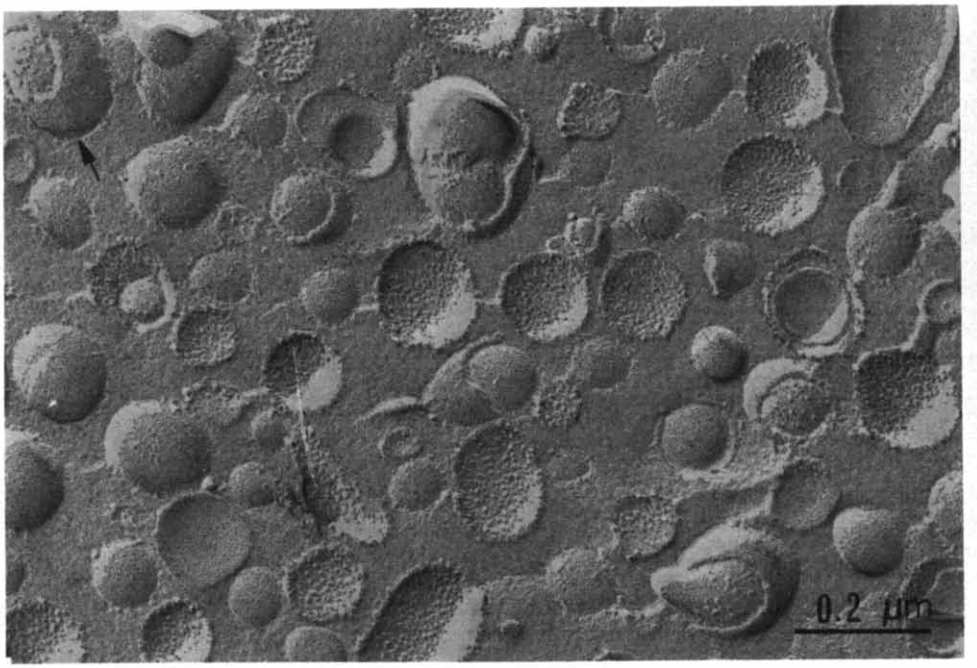

Fig. 2. Electron micrograph of freeze-fracture replica of the gastric microsomes. Gastric microsomes were concentrated to a pellet by centrifugation, frozen and fractured as described in Methods. The majority of vesicles appeared spherical with diameters of from 1000 to 2000 Å. Many of them were covered with particles 60—90 Å in diameter. The distribution of these intramembraneous particles was asymmetric with the concave faces mostly particulate while the convex faces are relatively smooth. Occasionally, some structures were seen with particulate convex surface within a smooth convex surface (arrow). These are interpreted to be due to the fracturing of an inside-out vesicle within a right-side-out vesicle. Magnification ×90 000.

reticulum vesicles, and the particles have been identified as the Ca^{2+}-ATPase [25—27]. Careful examination of Fig. 2 shows that some vesicles appear to have a particulate convex surface within a smooth convex surface. This may be due to the fracturing of an inside-out vesicle within a right-side-out vesicle, or this may be due to the fracturing of a horseshoe-type of vesicle. Both types of structures can be seen in electron micrographs of negatively stained preparations [16].

Effects of pH and [K^+]

Previous studies on the gastric K^+-ATPase have suggested the optimal enzyme activity occurred at pH 7.0—7.5 [3,16], with K_a for K^+ activation showing marked variation amongst the various animal species used to prepare the microsomes [28]. For all species there was an inhibition of ATPase activity as [K^+] was elevated to 10 times or greater than the apparent K_a [16,28]. These latter observations seemed to be at variance with data from Sachs' laboratory [2,5] and our own [14] showing that maximal H^+ transport activity occurred at high KCl concentrations, e.g. 150 mM. Thus, we initiated a systematic study varying both [K^+] and pH so as to establish optimal conditions for K^+-ATPase, the effects of valinomycin and the vesicular accumulation of H^+.

For convenience we will refer to the various ATPase activities in the following ways: Mg^{2+}-ATPase is that which occurs in the absence of K^+; K^+-stimulated ATPase is the activity which occurs in the presence of K^+ minus Mg^{2+}-ATPase activity; and the increment in K^+-ATPase activity produced by the addition of valinomycin is referred to as the valinomycin-stimulated K^+-ATPase.

The effects of KCl on ATPase activity are shown in Fig. 3 for several conditions of bulk medium pH. K^+-stimulated ATPase activity had highest activity at pH 7.1 and at relatively low $[K^+]$; however, a number of complexities dependent upon pH, $[K^+]$ and the presence of valinomycin are exemplified in Fig. 3. The apparent K_a for K^+ activation tended to increase as the pH of the medium was decreased; but the inhibitory effects of high K^+, noted previously, were also diminished or absent at the lower pH conditions. Addition of valinomycin caused stimulation of K^+-ATPase in most cases with optimal activity of the valinomycin-stimulated K^+-ATPase occurring at about pH 6.7. The apparent K_a for activation by K^+ of the valinomycin-stimulated ATPase was very high, with the system showing little or no saturation, especially at the lower pH values. Note that the Mg^{2+}-ATPase increased as the pH increased; optimal conditions for the Mg^{2+}-ATPase were not determined.

The results of parallel experiments assessing the effect of varying $[K^+]$ on the rate of acridine orange uptake and ATPase are shown in Fig. 4. An approximately linear relation exists between the rate of acridine orange uptake and $[K^+]$, up to 150 mM (Fig. 4A). The K^+ dependence for ATP hydrolysis in the presence and absence of valinomycin, as well as the difference between these two conditions is shown in Fig. 4B. It can be seen that only the valinomycin-stimulated K^+-ATPase has approximately linear behavior. This would support the view that it is primarily the valinomycin-stimulated part of the ATPase that is significantly contributing to the generation of the H^+ gradient.

A comparison of K^+-ATPase activities and vesicular H^+ gradient formation as a function of external medium pH is shown in Fig. 5. Optimal activity for acidifying the vesicular interior occurred when the extravesicular pH was about 6.6. K^+-stimulated ATPase activity showed a broad pH optimum; again stimula-

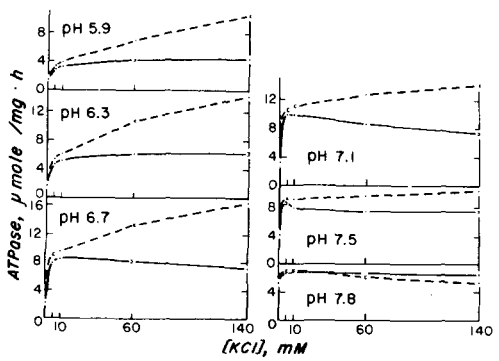

Fig. 3. Effect of KCl concentration on ATPase activity of gastric microsomal vesicles at several conditions of medium pH. The range of duplicate measurements is shown by the height of the point at each K^+ concentration. ———, ATPase without ionophore; - - - - - -, with $1 \cdot 10^{-5}$ M valinomycin.

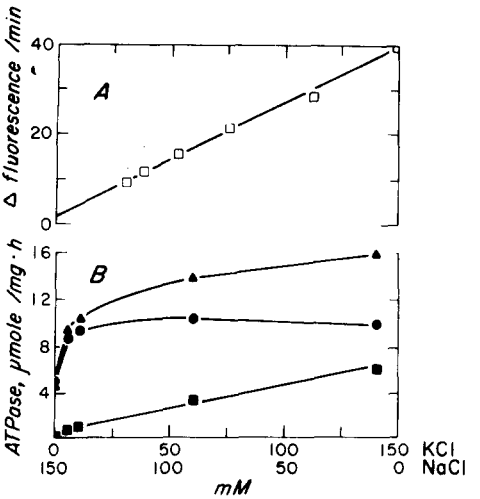

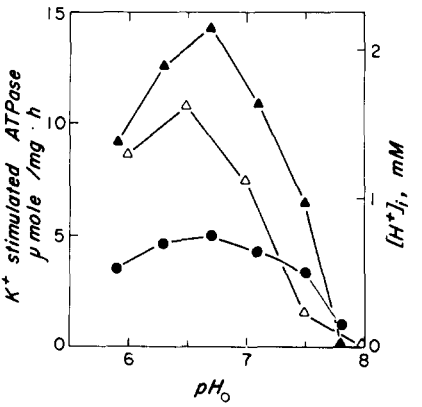

Fig. 4. The effect of $[K^+]$ on the initial rate of acridine orange fluorescence quenching and on the ATPase activity. A, The reaction medium contained 1 mM $MgSO_2$, 2.5 μM valinomycin, 5 μM acridine orange, and 10 mM Pipes (pH 6.5). $[K^+]$ was varied from 30 to 150 mequiv./l. The $[Cl^-]$ was kept constant at 150 mequiv./l with varying amounts of NaCl as indicated in the figure. The reaction was started with the addition of 0.5 mM ATP. B. The reaction medium contained 1 mM $MgSO_4$ and 10 mM Pipes (pH 6.5). The $[K^+]$ was varied as described in A. ATPase was measured in the presence of (▲) or absence (●) of $1 \cdot 10^{-5}$ M valinomycin. The difference between these conditions is shown as the valinomycin-stimulated K^+-ATPase (■).

Fig. 5. pH profile of K^+-ATPase activities and H^+ gradient formation by gastric vesicles. ATPase was measured in the presence of 140 mM KCl at the bulk medium pH_0 as indicated, with (▲) or without (●) $1 \cdot 10^{-5}$ M valinomycin. The internal H^+ concentration ($[H^+]_i$, △) was calculated from 9-aminoacridine uptake as previously described [14]. The maximum amount of dye uptake was measured as the percentage of total fluorescence intensity quenched in 150 mM KCl and 1 mM $MgSO_4$ at the various pH_0 as indicated with 0.14 mg protein/ml gastric microsomes, 10 μM valinomycin, 10 μM 9-aminoacridine and 1 mM ATP.

tion of K^+-ATPase by valinomycin was pronounced with optimal activity occurring at about pH 6.7. A summary of ATPase activity measurements on several different preparations of membranes carried out at pH 6.7 and 140 mM KCl is shown in Table I.

The time course of simultaneous measurement of ATP hydrolysis and uptake of 9-aminoacridine by the gastric microsomes under identical conditions is shown in Fig. 6. Addition of ATP to microsomes, in the presence of K^+ and Mg^{2+}, initiated ATP hydrolysis (Fig. 6A), but only a minimal amount of dye uptake occurred and tended to level off after the first 2 min (Fig. 6B). Addition of valinomycin stimulated the rate of ATP hydrolysis, and the dye uptake was dramatically increased.

In order to explain the role of valinomycin in stimulating the K^+-ATPase, we refer to the model system of Fig. 1 and suggest that the rate of penetration of K^+ to an internal activating site is rate limiting for the microsomal ATPase, a constraint that is largely relaxed when valinomycin is included in the incubation mixture. Valinomycin increases the permeability of intact vesicles to K^+, but K^+ entry must be electrically coupled to H^+ efflux and/or to the co-entry of an anion (Cl^- in this case). Since the results show that valinomycin stimulation

TABLE I

ATPase ACTIVITIES OF GASTRIC MICROSOMES

ATPase activity was measured for a number of different microsomal preparations (n) at room temperature (21—24°C) or 37°C at pH 6.5 as described in Materials and Methods, and reported as the mean ± S.E. All assays included 1 mM ATP and 1 mM $MgSO_4$, with KCl and valinomycin being included as indicated.

	ATPase (μmol $P_i \cdot mg^{-1}$ protein $\cdot h^{-1}$)	
	Room temperature (n = 10)	37°C (n = 6)
Mg^{2+} alone	2.68 ± 0.32	5.98 ± 0.46
140 mM KCl	7.46 ± 0.56	23.6 ± 2.49
140 mM KCl plus $1 \cdot 10^{-5}$ M valinomycin	17.15 ± 1.39	60.8 ± 8.45

of ATPase is also associated with H^+ uptake, we conclude that the anion influx pathway must be important for the operation of the system. We would postulate that most of the ATP hydrolyzed in the absence of valinomycin is not contributing to the creation of the H^+ gradient. This hydrolysis may be due to, for example, broken or leaky vesicles and therefore non-productive. In the presence of permeable anions, valinomycin would promote the accessibility of K^+ to some intravesicular pump sites of those tight vesicles and activate more ATP hydrolysis which is also productive in terms of a K^+/H^+ exchange pump.

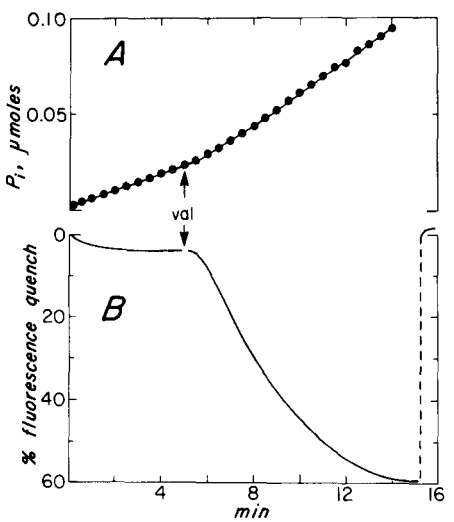

Fig. 6. Time course of ATP hydrolysis and the quenching of 9-aminoacridine by gastric microsomal vesicles. Gastric microsomes (76 μg protein/ml) were placed in a medium of 150 mM KCl, 1 mM $MgSO_4$ and 10 mM Pipes buffer (pH 7.0). A. ATP hydrolysis was measured after addition of 1 mM ATP by sampling timed 0.5 ml aliquots and assaying for P_i. Measured rates of ATPase activity before and after the addition of 10 μM valinomycin (val) were 6.8 and 13.8 μmol $\cdot mg^{-1} \cdot h^{-1}$, respectively. B. A 2 ml sample of the same preparation was placed in a cuvette with 10 μM 9-aminoacridine and the fluorescence intensity, measured at 455 nm immediately after adding 1 mM ATP, was taken as 100%, i.e. zero percent quenching (excitation, 422 nm). Changes in fluorescence intensity were measured continuously over the same time course as in A and are taken to indicate formation of a vesicular H^+ gradient. The addition of 5 μM nigericin at the end of the experiment (- - - - -) abolished the H^+ gradient.

Hence dramatic dye uptake occurs as the result of the formation of a larger H^+ gradient. The minimal amount of dye uptake before the addition of valinomycin might be due to the low, but finite, permeability of the vesicular membrane to K^+ allowing some K^+ access to the internal sites.

Effect of anions

Since our proposal for optimal vesicular H^+ uptake and K^+-ATPase activity suggests a limiting role for the rate of anion permeation, we wished to study the influence of various anions on the system. Experiments were first conducted at a constant $[K^+]$ of 140 mequiv./l with reciprocal variation of the anion; anions tested included Br^-, Cl^-, I^-, acetate, isethionate and SO_4^{2-}. A typical experiment on ATPase activity in which acetate was substituted for Br^- is shown in Fig. 7. In the absence of K^+ ionophore, as $[Br^-]$ was increased there was only a slight increase in ATPase activity; whereas the effects of Br^- are quite marked in the presence of valinomycin. Similar results were seen when isethionate was substituted for Br^- or Cl^-. The rather small stimulation of K^+-ATPase by valinomycin in potassium acetate or potassium isethionate media may be due to the limited permeability of the respective anions. Thus, the flux of K^+ into some activating site within the vesicles would be limited by the counterion movement, either an accompanying anion influx or H^+ exchange efflux. Support for this interpretation comes from experiments in which the anions were varied in a system where K^+ and H^+ permeability were concomitantly increased. As exemplified in Fig. 7, when both valinomycin and a protonophore were included, or when the neutral exchange ionophore, nigericin, was used, K^+-ATPase activity was markedly stimulated in the acetate (or isethionate) solutions, with only rather small increments being observed as Br^- or Cl^- were used as replacement anions.

The effect of $[Br^-]$ on acridine orange uptake is shown in Fig. 8. In the presence of K^+, Mg^{2+}, ATP and valinomycin, the rate of H^+ uptake, as evidenced from dye uptake, increased as $[Br^-]$ was increased in substitution for acetate. The correlation between H^+ uptake and ATPase activity may explain the importance of Br^-, or any permeable anion, for H^+ uptake. According to

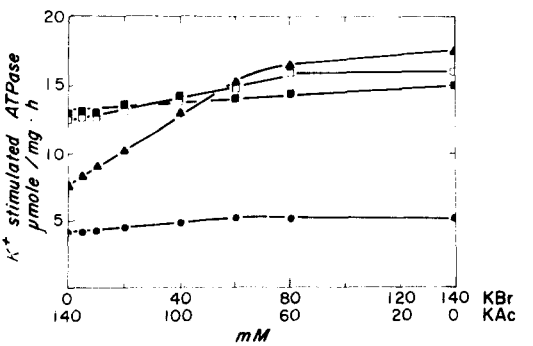

Fig. 7. Gastric vesicle ATPase activity under conditions where Br^- and acetate were reciprocally varied at a constant $[K^+]$ of 140 mequiv./l. ATPase activity without ionophore (●), in the presence of $1 \cdot 10^{-5}$ M valinomycin (▲), with $1 \cdot 10^{-6}$ M nigericin (■), and in the presence of $1 \cdot 10^{-5}$ M valinomycin plus $1 \cdot 10^{-6}$ M TCS (□).

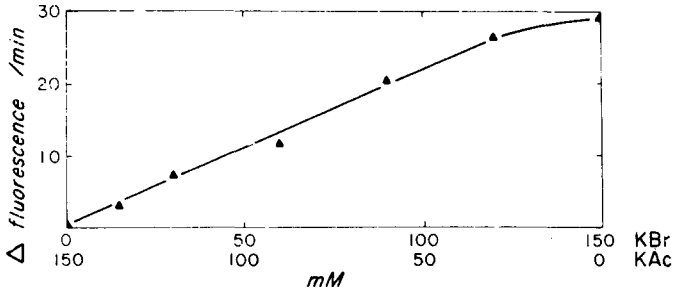

Fig. 8. Effect of Br^- concentration of the initial rate of acridine orange fluorescence quenching at a constant $[K^+]$ of 150 mequiv./l. The Br^- concentration was increased in substitution for acetate. In addition, the reaction medium contained 5 μM acridine orange, 10 mM Pipes buffer (pH 6.5), 1 mM $MgSO_4$, 60 μg/ml membrane protein and 2.5 μM valinomycin. The sample was excited with 493 nm light and the fluorescence monitored at 530 nm. After addition of 1 mM Na-ATP, the initial rate of fluorescence quenching was measured at room temperature.

the scheme shown in Fig. 1, H^+ accumulation would occur as the pump exchanges K^+ for H^+. Effective pump activity would thus depend on the availability of internal K^+ which would in turn be provided by K^+ entry (valinomycin) in the presence of permeable anions. The pump would also be stimulated by addition of K^+/H^+ exchange ionophores, but would be essentially uncoupled from H^+ accumulation since the proton loss would occur rapidly through the high leak pathway.

Following the above line of reasoning, we could compare the effects of a variety of anions on the gastric microsomal ATPase and H^+ accumulation activities. Results for K^+-ATPase are shown in Table II. The differences in ATPase activity were relatively small for the various anions in the absence of ionophore or during conditions of high K^+/H^+ exchange (valinomycin plus TCS, or nigericin) where anion entry might be less rate limiting. In the presence of

TABLE II

EFFECT OF VARIOUS ANIONS ON K^+-ATPase ACTIVITY

ATPase values are given in μmol $P_i \cdot mg^{-1}$ protein $\cdot h^{-1}$ as the mean ± S.E. of four measurements, except where indicated. Microsomal vesicles were incubated with 140 mM potassium salts of various anions, as indicated, for the standard ATPase assay including 1 mM ATP, 1 mM $MgSO_4$, and 10 mM Pipes buffer at pH 6.7. The basal ATPase in the absence of K^+ was 2.3 ± 0.21 μmol $P_i \cdot mg^{-1}$ protein $\cdot h^{-1}$. Concentrations of ionophores were: valinomycin, $1 \cdot 10^{-5}$ M; nigericin, $1 \cdot 10^{-6}$ M; and TCS, $1 \cdot 10^{-6}$ M. Separate experiments verified that these ionophore concentration produced maximal effects; higher concentration of ionophores were inhibitory.

	KBr	KCl	KI *	Potassium acetate	Potassium isethionate
No ionophore	4.83 ± 0.06	4.26 ± 0.08	5.63 ± 0.12	3.55 ± 0.14	3.30 ± 0.12
Valinomycin	15.98 ± 0.22	12.75 ± 0.48	8.99 ± 0.12	6.62 ± 0.24	6.57 ± 0.15
Valinomycin plus TCS	15.17 ± 0.52	13.04 ± 0.31	10.44 ± 0.12	11.96 ± 0.18	9.50 ± 0.85
Nigericin	15.54 ± 0.29	13.27 ± 0.86	13.13 ± 0.03	13.06 ± 0.37	10.92 ± 0.93
Nigericin plus valinomycin	18.90 ± 1.02	17.54 ± 0.86	16.65 ± 0.01	12.18 ± 0.58	10.83 ± 0.11
TCS *	4.26 ± 0.02	4.84 ± 0.46	6.11 ± 0.02	4.26 ± 0.02	2.68 ± 0.08

* Values are presented as the mean of only two separate measurements.

valinomycin alone, marked differences occurred with the order of stimulation being $Br^- > Cl^- > I^- >$ acetate > isethionate. (Tests with SO_4^{2-} also showed that this anion fit into the low permeability category, but because of some secondary inhibitory effects of SO_4^{2-} on enzyme activity the data are not included.) Thus, the rate-limiting step for valinomycin-stimulated ATPase activity appears to be the degree of anion permeation which would accompany K^+ to the activating site. When valinomycin and nigericin were present together, ATPase activity was even further stimulated with the same order of anion activity as observed for valinomycin alone. This would suggest that enzyme activity is still dependent upon the rate of K^+ entry under these conditions, which in turn show the anion limitation; thus the turnover of the enzyme can be increased through both the K^+/H^+ exchange and K^+/anion entry pathways.

A comparison of the anions in promoting H^+ uptake is shown in Fig. 9. The order of selectivity for various anions tested in the presence of valinomycin is $NO_3^- > Br^- > Cl^-$ > acetate ≈ isethionate. (Experiments with I^- place this anion between Cl^- and acetate, but some independent effect of I^- in quenching acridine orange make the data quantitatively unreliable.) Additions of protonophores (TCS or CCCP) or nigericin on top of valinomycin leads to rapid dissipation of the H^+ gradient for all anions.

Effects of SCN^-

SCN^- was an interesting anion to test because of its well-known inhibitory effects on HCl secretion and because of its action as a chaotropic ion in several membrane systems. It turns out that the effects of SCN^- on this system must

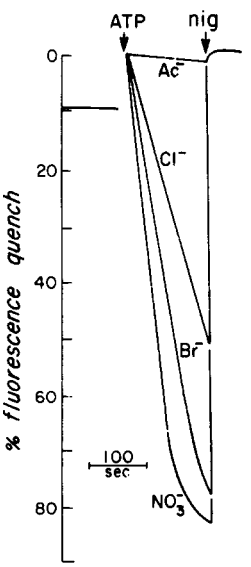

Fig. 9. The effect of several K^+ salts on acridine orange uptake by gastric vesicles. A higher degree of fluorescence quenching represents higher uptake of acridine orange into the vesicles, which, in turn, indicates a lower pH inside the vesicles. The conditions in this experiment are identical to those of Fig. 8 with the exception of the substitution of the major anion. The use of isethionate and SO_4^{2-} as the major anion (not shown) produced results identical to acetate (Ac^-).

be interpreted with caution. Our preliminary tests showed an apparent inhibition of the valinomycin-stimulated, K^+-ATPase activity when 5—15 mM SCN^- was added to membranes with KCl or KBr, and a slight stimulation in the presence of potassium acetate. We have since found this to be a phenomenon of interaction between SCN^- and valinomycin (or valinomycin-K^+ complex) in free solution. When SCN^- was allowed to incubate with valinomycin prior to addition of membranes, there was an 'inactivation' of valinomycin as an ionophore. (Another chaotropic anion, ClO_4^-, is even more effective than SCN^- in the 'inactivation' of valinomycin.) This inactivation process has a $t_{1/2}$ of about 10 min at 22° C using 10 mM SCN^-. However, if valinomycin is incubated with membranes prior to adding SCN^-, the partitioning of the ionophore within the membranes allowed maintained function for long periods of time (up to 1 h). An exemplary experiment is shown in Table III which compares the effects of 10 mM NaSCN added to the membranes prior to and after the addition of valinomycin. When SCN^- was preincubated with valinomycin for 30 min prior to adding the membranes, ATPase was markedly inhibited in the KBr or KCl media with relatively little effect for potassium acetate. When membranes were first preincubated with valinomycin, the subsequent addition of SCN^- had little effect when the major salt was KBr or KCl, while there was marked stimulation of ATPase activity in the potassium acetate medium. Higher concentrations of SCN^- (>15 mM) tended to reduce K^+-ATPase activity toward the levels observed without ionophore.

An additional set of experiments were designed to test the relative effect of SCN^- and other anions on the valinomycin-stimulated K^+-ATPase. As shown in Table IV, the various anions were added as the Na^+ salt (10 mM) on top of membranes incubated in 140 mM potassium acetate, with or without valinomycin. The order of activation was $SCN^- > NO_3^- > Br^- > Cl^-$ > acetate.

Correlations of vesicular H^+ transport with K^+-ATPase activity

ATP. K_m values for ATP was obtained from the Lineweaver-Burk plot for the ATPase activities as shown in Fig. 10A. ATPase activities were measured in

TABLE III

EFFECT OF SCN^- ON GASTRIC K^+-ATPase

In one case, 10 mM NaSCN was preincubated with $1 \cdot 10^{-5}$ M valinomycin in the assay medium for 30 min prior to adding membranes. In the other case, membranes and valinomycin were preincubated before adding the 10 mM NaSCN. Basal ATPase activity (in absence of K^+) was 2.0 $\mu mol \cdot mg^{-1} \cdot h^{-1}$.

	ATPase activity ($\mu mol \cdot mg^{-1} \cdot h^{-1}$)		
	Potassium acetate (140 mM)	KCl (140 mM)	KBr (140 mM)
No addition	3.1	5.0	4.3
Valinomycin ($1 \cdot 10^{-5}$ M)	5.7	14.2	17.3
Valinomycin plus SCN^- preincubated prior to adding membranes	5.6	7.3	7.0
Valinomycin plus membranes preincubated prior to adding SCN^-	11.8	15.1	16.6

TABLE IV

THE EFFECT OF VALINOMYCIN (OR NIGERICIN) IN STIMULATING K^+-ATPase ACTIVITY IN THE PRESENCE OF 10 mEquiv./L OF VARIOUS ANIONS

Reaction tubes were prepared with 140 mM potassium acetate, 10 mM Pipes buffer (pH 6.7), 1 mM $MgSO_4$, 25 μg membrane protein, with or without $1 \cdot 10^{-5}$ M valinomycin or $1 \cdot 10^{-6}$ M nigericin. 10 mM of the K^+ salt of the indicated anion was then added, and the reaction subsequently initiated by adding 1 mM ATP. Results are reported as the mean ± S.E. of four measurements, except for experiments with nigericin where only two measurements were carried out.

	K^+-ATPase activity (μmol $P_i \cdot mg^{-1}$ protein $\cdot h^{-1}$)				
	SCN^-	NO_3^-	Br^-	Cl^-	Acetate
No ionophore	3.89 ± 0.08	3.70 ± 0.09	3.36 ± 0.05	3.49 ± 0.02	3.03 ± 0.08
Valinomycin	10.40 ± 0.92	8.26 ± 0.22	7.76 ± 0.25	6.69 ± 0.19	5.60 ± 0.21
Nigericin	13.89 ± 0.29				11.44 ± 0.11

the presence of K^+ alone and in the presence of K^+ plus valinomycin; estimated K_m values were 77 μM and 56 μM ATP, respectively. The difference between these two activities, or the valinomycin-stimulated ATPase activity, gave a K_m of 50 μM. As can be seen from the figure, all ATPase data gave reasonably good fits to linearity. In Fig. 10B, the double-reciprocal plot of ATP vs. the initial rates for acridine orange uptake is shown. There is reasonable linearity at the lower range of ATP concentration with an apparent K_m of 50 μM in close correspondence with the valinomycin-stimulated ATPase. Deviation from linearity in the high [ATP] region would not likely be substrate inhibition since the pump enzyme was not similarly affected. It may, however, be related to the fact that acridine orange uptake is related to the pH gradient across the microsomal membranes, which, in turn, is related to the balance between the pump and the leaks.

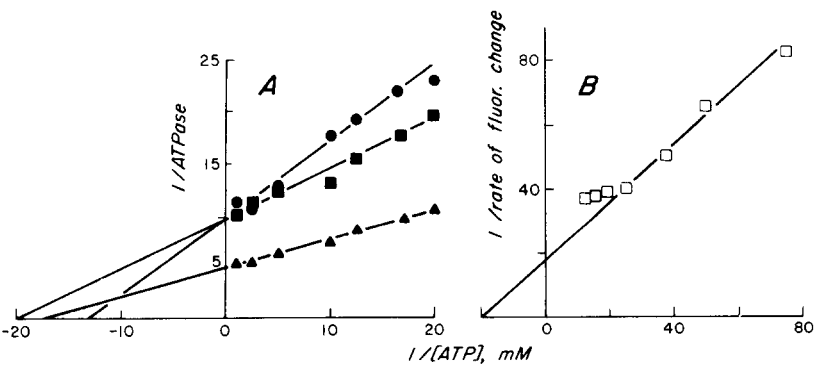

Fig. 10. Kinetics of ATP on the activation of gastric microsomal ATPase and the rate of acridine orange uptake plotted according to Lineweaver-Burk. A. ATPase activity was measured as described in Fig. 4B, with 20 μg protein/ml of gastric microsomes. The K^+-stimulated ATPase is shown in the absence (●) and presence (▲) of $1 \cdot 10^{-5}$ M valinomycin. The difference between these values is shown as the valinomycin-stimulated K^+-ATPase (■). B. The rate of acridine orange uptake was measured by the spectrofluorimetric method as the rate of fluorescence quenching in the same medium as above, including 50 μg/ml gastric microsomes, 5 μM acridine orange and 2.5 μM valinomycin.

Effects of temperature. In Fig. 11A an Arrhenius plot for the rate of acridine orange uptake in the presence of valinomycin is shown. There is a clear break at about 16° C. The activation energy was calculated to be 21 kcal/mol above the break and 40 kcal/mol below. The Arrhenius plots for the Mg^{2+}-ATPase, K^+-stimulated ATPase and valinomycin-stimulated K^+-ATPase are shown in Fig. 11B. Both the Mg^{2+}-ATPase and valinomycin-stimulated ATPase have a break at about 14° C, but for the K^+-ATPase there was no apparent break in the Arrhenius plot. The activation energies for the Mg^{2+}-ATPase were calculated to be 14 kcal/mol above the break and 37 kcal/mol below; for the K^+-stimulated ATPase, it was 16 kcal/mol; for the valinomycin-stimulated ATPase, activation energies were 19 kcal/mol above the break and 45 kcal/mol below the break. Thus, a rather good correlation exists between valinomycin-stimulated ATPase and the dye uptake, both in terms of having a break around the same temperature and the consistent activation energies above and below the break. This break in the Arrhenius plot has been observed in many other enzyme system [29—31] and has frequently been attributed to some phase transition of the lipoid membrane components.

Sulfhydryl reagents. The effect of MalNEt treatment on the ATPase activities is shown in Fig. 12A. Both the Mg^{2+}-ATPase and the K^+-ATPase are very resistant to the treatment. For instance, after 90 min of reaction with 10 mM MalNEt, there was essentially no change in Mg^{2+}-ATPase and only a slight decrease in K^+-ATPase. However, the valinomycin-stimulated ATPase was highly sensitive to MalNEt and was essentially eliminated after 30 min of reaction. In Fig. 12B, the percentage of inhibition of the valinomycin-stimulated ATPase (compared to no MalNEt treatment) was plotted against the length of time of the reaction with MalNEt. In the same figure, the time course of inhibition of the rate of acridine orange uptake is also presented. The similarity between the two curves is obvious.

The kinetics of reaction of microsomal membranes with another SH reagent, DTNB, can be easily resolved by graphical analysis into three phases as described in Materials and Methods. Each phase is characterized by a rate constant and is listed in Table V, together with the number of SH groups/mg of protein for each phase. The results presented in Table V were obtained by reaction with DTNB in 150 mM KCl (high ionic strength), pH 8.0. Similar results were obtained by replacing KCl with NaCl. However, in low ionic strength medium (e.g. homogenizing medium, pH 8.0), the fastest phase was dramatically reduced (approx. 80%) and only the medium and slow phases were left. It thus appears that there are some structural rearrangements induced by the ionic strength of the medium. In Fig. 13, the time course of the effect of DTNB reaction on the ATPase activity is shown. Similar to the results for MalNEt treatment, the K^+-ATPase was resistant to DTNB, while the valinomycin-stimulated ATPase was much more sensitive and was reduced to zero after 1 h incubation with 0.4 mM DTNB. Consistent with absorbance measurements, three phases can also be seen in the time course for inhibition of the valinomycin-stimulated ATPase.

Unlike DTNB and MalNEt, we have found that *p*-chloromercuribenzenesulfonate ($1 \cdot 10^{-5}$ M) produced an effective and non-selective inhibition of ATPase activity in the sense that it inhibits Mg^{2+}-ATPase, K^+-stimulated ATPase

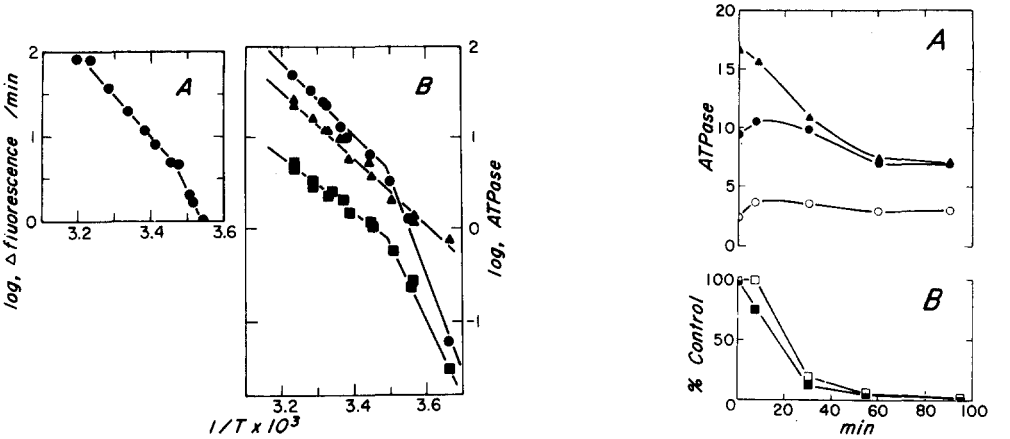

Fig. 11. Arrhenius plot of the rate of acridine orange uptake and the ATPase activity. A. Acridine orange uptake was measured by the spectrofluorimetric method as the rate of fluorescence quenching in K^+/Mg^{2+} medium (pH 6.5) with 0.035 mg protein/ml gastric microsomes, 2.5 μM valinomycin and 5 μM acridine orange. Temperature was varied from 9 to 40°C. B. The basal Mg^{2+}-ATPase activity was measured in a medium containing 10 mM Pipes (pH 6.5), 1 mM $MgCl_2$ and 1 mM ATP (■). K^+-stimulated ATPase (▲) was measured as the increase over the basal activity produced by 140 mM KCl. Addition of 10 μM valinomycin produced a further stimulation which is plotted as the valinomycin-stimulated K^+-ATPase (●). Temperature was varied from 4 to 37°C.

Fig. 12. Effects of SH-group modification with *N*-ethylmaleimide (MalNEt) on the ATPase activity and the rate of acridine orange uptake. Gastric microsomes (1.12 mg protein/ml) were reacted with 10 mM MalNEt for various periods of time, as indicated, and the treatment was terminated by dilution as described in Methods. A. The treated microsomes were assayed for ATPase activity in the presence of 1 mM $MgSO_4$, 1 mM ATP and 10 mM Pipes at pH 6.5. Results are presented for the basal Mg^{2+}-ATPase (○); in the presence of both Mg^{2+} and 150 mM KCl (●, K^+-ATPase); and in the presence of Mg^{2+}, K^+ and 10 μM valinomycin (▲, valinomycin-ATPase). B. The time course of inhibition is shown for the valinomycin-stimulated K^+-ATPase (■, valinomycin-ATPase minus K^+-ATPase) and acridine orange uptake activity (□) of the MalNEt-treated microsomes described in A. The rate of acridine orange uptake was measured as described in Fig. 10. Both the ATPase and the dye uptake data are plotted as percentage of the zero time value.

TABLE V

NUMBER OF SULPHYDRYLS (AND THEIR RATE CONSTANTS) IN EACH KINETIC SET FOR THE MODIFICATION OF GASTRIC MICROSOMES WITH DTNB

Gastric microsomes (0.4 mg protein/ml) were reacted with 0.4 mM DTNB in K^+/Mg^{2+} medium (pH 8.0). The absorbance change was monitored continuously in a dual wavelength spectrophotometer using 412 nm as sample and 500 nm as reference wavelengths. Three sets of kinetically distinguishable sulfhydryls (fast, medium and slow) were obtained from graphical analysis of the absorbance data as described in Materials and Methods. Number of sulfhydryls, n, in each kinetic set is expressed as nmol/mg membrane protein; pseudo-first order rate constants, k_1, are in units of min^{-1}. Unreactive was calculated by subtracting the sum of the reactive groups from the total found in the presence of 0.5 mM sodium dodecyl sulfate.

	Fast	Medium	Slow	Unreactive
n	14.5	8.1	27.6	30.0
k_1	9.0	1.4	0.33	—

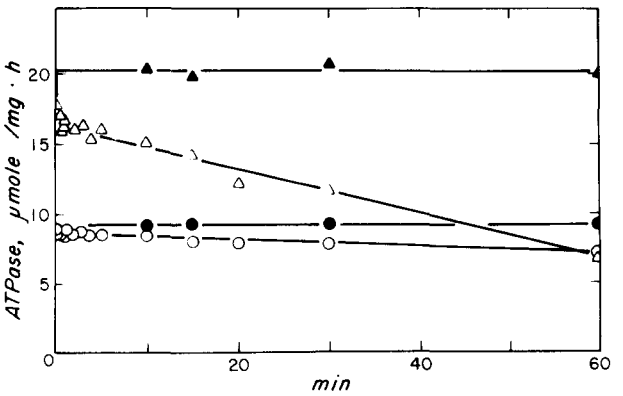

Fig. 13. Time course for the inhibition of the ATPase activity by DTNB treatment. Gastric microsomes (0.53 mg/ml) were treated with 0.4 mM DTNB in K^+/Mg^{2+} medium (pH 8.0) for the indicated periods of time. The DTNB reaction was terminated by the addition of 0.8 mM cysteine. The treated microsomes were assayed for ATPase activity in K^+/Mg^{2+} medium, pH 6.5, with (△) or without (○) 10 μM valinomycin. Control values were obtained for microsomes treated identically but without DTNB in the presence (▲) and absence (●) of 10 μM valinomycin.

and valinomycin-stimulated ATPase, and works almost instantaneously. This same instantaneous inhibition was also observed in the dye uptake and can be partially reversed by the addition of cysteine. These observations with *p*-chloromercuribenzenesulfonate are in conformance with earlier reports of others [5].

Amino group modification. Fig. 14A shows the inhibitory effects of amino group modification. Similar to the SH-group reagents, DTNB and MalNEt, the monofunctional imidoester, ethylacetimidate, selectively inhibited the ionophoretic-stimulated part of the ATPase. After 15 min of incubation with 20 mM ethylacetimidate, the gramicidin-stimulated part of the ATPase was completely abolished, but the K^+-stimulated ATPase and Mg^{2+}-ATPase were essentially unaffected. Acridine orange uptake was also inhibited with a similar time course. The bifunctional imidoester, dimethylsuberimidate, was much more effective in inhibiting the ATPase than the monofunctional ethylacetimidate. As can be seen, after only 5 min of incubation the gramicidin-stimulated ATPase was eliminated, and also both K^+-stimulated ATPase and Mg^{2+}-ATPase showed some inhibition. In a study of the time course of reactivity (Fig. 14B), we found that although the number of amino groups that reacted with dimethylsuberimidate is less than with ethylacetimidate, the inhibition of the ATPase is higher. This may indicate that conformational change or mobility of the enzyme is important for the enzymatic reaction which, of course, should be more effectively inhibited by a cross-linker like dimethylsuberimidate than by monofunctional reagents. Indeed, with the use of SDS gel electrophoresis, it was observed (data not shown) that after 5 min reaction with 20 mM dimethylsuberimidate, virtually all protein molecules were cross-linked to such a high molecular weight that they were not able to enter the gel.

Other inhibitors. In previous reports, we have shown that Zn^{2+} and F^- are effective inhibitors of K^+- and K^+ ionophore-stimulated ATPase activity [28,32]. We have confirmed these results and have observed in parallel experi-

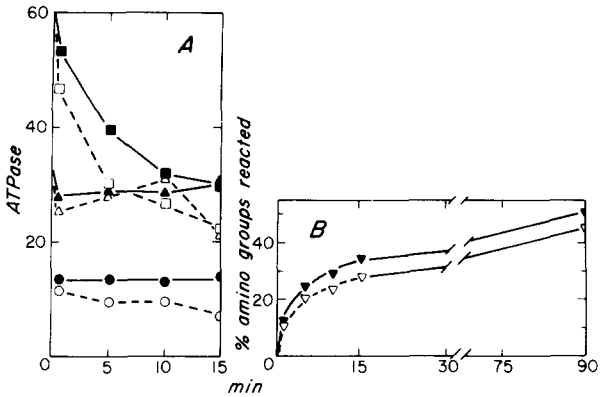

Fig. 14. Effects of amino-group modification on the ATPase activity. A. Gastric microsomes (0.5 mg protein/ml) were treated with either 20 mM ethylacetimidate (EA) or 10 mM dimethylsuberimidate (DMS) for the indicated periods of time as described in Methods and the reaction was terminated by dilution in cold 100 mM Tris buffer (pH 7.5). Results are shown for the basal Mg^{2+}-ATPase (●, EA and ○, DMS); in the presence of Mg^{2+} and 10 mM KCl (▲, EA and △, DMS); and in the presence of Mg^{2+}, K^+ and 10 μM gramicidin (■, EA and □, DMS). B. The amount of free amino groups on the gastric microsomes after reaction with EA (▲) and DMS (△) for the indicated periods of time was assayed by the fluorescamine method. 0.1 ml microsomes, reacted as described in A, were added to 1.5 ml 0.2 M sodium borate buffer (pH 9.0) and 0.5 ml fluorescamine (0.15 mg/ml acetone) was added. Fluorescence intensity at 480 nm (excited at 390 nm), which is proportional to the amount of free amino groups on the microsomes, was measured. Control values were obtained with untreated microsomes.

ments that Zn^{2+} and F^- also inhibit dye uptake. As described earlier [32], F^- is an interesting case requiring some preincubation with membranes. Thus 1 mM NaF inhibits about 60% of the K^+-ATPase and valinomycin-ATPase after 5 min of preincubation at room temperature, with 20 min of preincubation being required for complete inhibition. A similar time course of inhibition was also observed for acridine orange uptake.

Discussion

The freeze-fracture images of the isolated gastric microsomes are consistent with earlier reports suggesting the vesicular nature of this preparation [1–6,14]. Moreover, the general organization of intramembraneous particles on the fracture faces occurs in the same pattern as that seen on the fracture planes of the tubulovesicular system from intact oxyntic cells [33]. It had been pointed out that the concave P face of tubulovesicles was very rich in membrane particles while the convex E face was smooth and virtually devoid of particles. For the isolated microsomal preparation, with the exception of those cases where the fracture planes revealed double membranous structures, the concave surfaces were rich with particles suggesting the analogy to the P face of tubulovesicles of intact tissue while the smooth convex surface was more consistent with the exterior or E face of the membrane. These results are thus consistent with immunocytochemical, ontogenetic and other studies which have suggested that these isolated gastric microsomes and their K^+-stimulated ATPase are derived from the tubulovesicular system of the oxyntic cell [2,16,34].

The specific identity of the intramembranous particles observed in the

gastric microsomes is not yet known. A protein of about 100 000 dalton size has been identified as the K^+-ATPase from phosphorylation and dephosphorylation studies using [γ-^{32}P]ATP [28,32]. The majority of protein of density gradient-purified hog gastric microsomes migrates on SDS gel electrophoresis in the 100 000 dalton region [16]; even further purification was achieved when the microsomes were prepared by free flow electrophoresis [5]. Thus, it is not unreasonable to postulate that the K^+-ATPase system is largely represented in the intramembranous particles of gastric vesicles, analogous to particles visualized and identified as the Ca^{2+}-ATPase on sarcoplasmic reticulum [26,27].

By using a series of activators and inhibitors, the present results add a strong measure of support to the notion that the gastric microsomal ATPase is positively correlated with H^+ transport activity. In particular, the valinomycin-stimulated part of the K^+-ATPase appears to correlate best with H^+ transport. The K^+-ATPase activity in the absence of valinomycin therefore largely represents non-productive ATP hydrolysis (i.e. in terms of H^+ transport). There are at least two possibilities to account for this latter type of K^+-ATPase activity: first, there is the possibility of a population of especially leaky or broken membrane vesicles; alternatively, we can propose the existence of two activation sites for K^+, one on the outside and one on the inside of the vesicles. The outside site might be responsible for non-productive ATP hydrolysis, while the inside site would be the pump site. Support for this latter interpretation comes from the fact that sulfhydryl reagents (MalNEt and DTNB) and amino group reagents selectively inhibit the valinomycin-stimulated part of the K^+-ATPase activity and, with the same time course, completely abolish the H^+ transport. This would suggest that the two sites have intrinsically different reactivity toward these inhibitors with the transport, or internal, site being more sensitive.

The present studies show that both the gastric K^+-stimulated ATPase activity and vesicular proton accumulation have clear anion-dependent effects. The dependence does not appear to be a direct enzymic effect, but can be explained almost entirely on the basis of the limiting rate of anion permeation across the vesicular membrane. According to several earlier proposals, the gastric K^+-stimulated ATPase is responsible for vesicular H^+ transport (accumulation) via a K^+/H^+ exchange process as depicted in Fig. 1. If K^+ were required at some deep intramembranous or intravesicular site, then the dependence of pump activity on both the K^+ and anion permeation rates is apparent. Accordingly, in the presence of K^+ ionophores (i.e. valinomycin) ATPase and pump activities are high with relatively permeant anions, such as NO_3^-, Br^- and Cl^-, and are relatively low in the case of acetate and isethionate. Under these conditions, pump activity would be coupled to the K^+ entry process with the latter, in turn, being modulated by the nature of the counterion.

For the cases where vesicular permeability was simulatneously increased to both K^+ and H^+ (e.g. nigericin or valinomycin plus TCS), the nature of the anion was less rate limiting for ATPase activity; however, the ability to accumulate protons, that is, effective pump activity, was abolished. This would suggest that high generalized cation permeability would represent a mechanism of uncoupling the ATPase activity from net proton accumulation, and the pump would be 'non-productive'. This would also explain earlier results which showed that gramicidin (an ionophore for both K^+ and H^+) was effective in

stimulating K^+-ATPase in KCl or potassium acetate media [16], while it dissipates the H^+ gradient.

Thiocyanate has long been known as a relatively effective and reversible inhibitor of gastric H^+ secretion. However, the present results with the K^+-stimulated ATPase of isolated gastric microsomal vesicles do not offer insight toward the mechanism by which thiocyanate may act in vivo. When inhibitory effects were observed, they were most likely the result of an interaction between thiocyanate and valinomycin, preventing the effective action of the K^+ ionophore. The fact that inhibition by thiocyanate can be seen when valinomycin was preincubated with thiocyanate would be consistent with the formation of ternary complex, valinomycin-K^+-thiocyanate, as suggested by several authors [35—37]. In egg lecithin liposomes, the turnover number of this ternary complex as a K^+ carrier [38] was at least 30 times less than the turnover number measured for the valinomycin-K^+ complex in black lipid membranes [39]. When our incubating conditions were such as to reduce the interactions between thiocyanate and valinomycin in free solution, thiocyanate up to 10 mM appeared to be relatively innocuous anion for both ATPase and proton pumping activities. In fact, from the relative rates of activation of the valinomycin-stimulated K^+-ATPase activities, it would appear that thiocyanate is a very permeant anion in agreement with results obtained by others [24].

The order of the halides in activating the microsomal H^+ transport activity, i.e. $Br^- > Cl^- > I^-$, is consistent with data for H^+ secretion by intact stomach [9], but the relative placement of both SCN^- and NO_3^- in this sequence does not fit the H^+ secretion data [9,40]. If the microsomal K^+-ATPase and H^+ pump were the primary mechanism for gastric H^+ transport, these variances must be explained. For intact mucosa, there might be other sites or mechanisms to account for inhibition or reduced transport (e.g. basolateral membrane, HCO_3^-/Cl^- exchange, metabolic effects, recycling of the anion), and these would have to be uncovered before we could specify the physiological role of the microsomal H^+ transport system.

A pump-leak model

The major findings described here add qualitative support to the scheme depicted in Fig. 1. We have extended the system to a more quantitative description of gastric vesicular function in the form of a pump-leak model. The first element in our model would be an ATP-driven K^+/H^+ exchange pump. For this active pathway, we used simple Michaelis-Menten kinetics with the substrate being internal $[K^+]$, and which transport n_H^K potassium ions out of the vesicle for each H^+ transported in. This is, of course, under conditions where other agents such as ATP and Mg^{2+} are not rate limiting. This pump can be either electroneutral ($n_H^K = 1$) or electrogenic ($n_H^K \neq 1$). The well-established Nernst-Planck formulation will be used to model passive pathways which are characterized by three permeability coefficients P_H, P_K and P_{Cl} for H^+, K^+ and Cl^-, respectively.

The mathematical derivations of the model are presented in the appendix. The time course of the changes of internal H^+, K^+ and Cl^- concentration is described by Eqns. 5, 6 and 7, respectively. The membrane potential is described by Eqn. 12. These four equations were solved numerically using a

PDP-11 minicomputer. In Fig. 15, the calculated internal concentration of H^+ was plotted against time under conditions where specific ionic permeabilities were varied. When P_K was low ($P_K = 1 \cdot 10^{-9}$ cm/min), the rate of H^+ transport was also low; $[H]_i$ increased only from $1 \cdot 10^{-7}$ to $5 \cdot 10^{-5}$ M in the first 4 min. An increase in P_K by two orders of magnitude to $1 \cdot 10^{-7}$ cm/min (which is taken as equivalent to addition of valinomycin to the gastric microsomes), dramatically increased H^+ transport, bringing $[H]_i$ to about $1 \cdot 10^{-2}$ M in a 10 min period (curve a, Fig. 15). When P_H was subsequently increased by two or three orders of magnitude (taken as equivalent to addition of a protonophore), there was a rapid dissipation of the H^+ gradient (curves a and a′ of Fig. 15). Curves b—d show the effect of decreasing P_{Cl}. As P_{Cl} was reduced from $1 \cdot 10^{-6}$ cm/min (curve a) to $1 \cdot 10^{-9}$ cm/min (curve d), the amount of

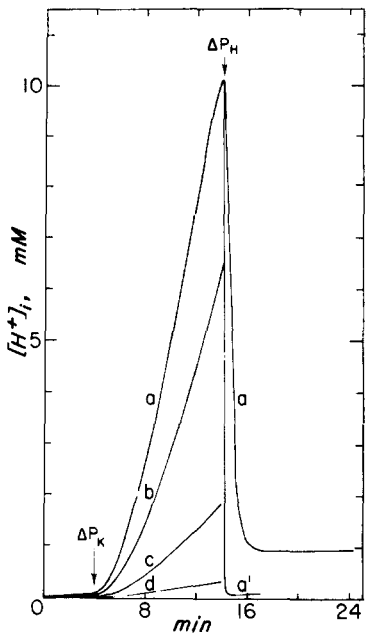

Fig. 15. Computer simulation of H^+ transport using the pump-leak model presented in the Appendix. In this model, the Nernst-Planck formulation was used as the description of the passive leak pathways characterized by three permeability coefficients: P_H, P_K and P_{Cl} for H, K^+ and Cl^-, respectively. For the modeling of the H^+ pump, simple Michaelis-Menten kinetics were used with the internal $[K^+]$ as substrate; for each turnover of the pump, n^H_{ATP} mol of H^+ were transported into the vesicles in exchange for n^H_{ATP} moles of K^+ out of the vesicles. The internal concentration of H^+ was calculated using Eqns. 5—7 and 12 of the Appendix. The values for the parameters used were as follows: $r = 1 \cdot 10^{-5}$ cm, $V_i = 2$ µl/mg, $n^H_{ATP} = 1$, $V_{Max} = 1 \cdot 10^{-8}$ mol/mg · min, $K_m = 0.1$ M, $n^H_K = 1$ and $F/RT = 0.39$/mV. The permeability coefficients used in curve a were $P_H = 1 \cdot 10^{-7}$ cm/min, $P_K = 1 \cdot 10^{-9}$ cm/min and $P_{Cl} = 1 \cdot 10^{-6}$ cm/min. At time $t = 4$ min (indicated by the arrow labeled ΔP_K), the P_K value was increased from $1 \cdot 10^{-9}$ to $1 \cdot 10^{-7}$ cm/min (this is taken as equivalent to addition of valinomycin). At time $t = 14$ min (indicated by the arrow labeled ΔP_H), the P_H value was increased to $1 \cdot 10^{-5}$ (curve a) or $1 \cdot 10^{-4}$ cm/min (curve a′) and is taken as equivalent to the addition of CCCP. For curves b—d, the P_{Cl} values were $1 \cdot 10^{-7}$, $1 \cdot 10^{-8}$ and $1 \cdot 10^{-9}$ cm/min, respectively. The ΔP_K for these three curves is the same as curve a. The initial conditions for internal ion concentrations were $[H_i] = 1 \cdot 10^{-7}$ M, $[Cl]_i = 1 \cdot 10^{-2}$ M and $[K]_i = 1 \cdot 10^{-6}$ M; and those of the external medium were $[H]_0 = 1 \cdot 10^{-7}$ M, $[Cl]_0 = 0.15$ M and $[K]_0 = 0.15$ M. These external values were assumed to be constant, independent of time.

enhanced H^+ transport due to the increase of P_K was also dramatically reduced. When $P_{Cl} = 1 \cdot 10^{-9}$ cm/min a subsequent increase in P_K has essentially no effect in stimulating H^+ transport.

The present pump-leak model is able to semi-quantitatively account for many of the experimentally observed ion transport properties of the microsomal system. In particular, it predicts the stimulation of H^+ uptake by valinomycin in the presence of permeable anions. It also predicts the dissipation of the H^+ gradient by the addition of protonophores on top of valinomycin. Finally, it shows that a reduction of anion permeability (e.g. replacement of permeable anion with an impermeable one) will eliminate the valinomycin stimulation. All these features, of course, were observed experimentally.

There are some shortcomings in the present form of the model. For instance, the pump term is based solely on the kinetic limitations imposed by K^+ availability to the pump site. It ignores the energetic limitations of the generated ion gradients in terms of the available driving force (i.e. ATP). This latter feature will be incorporated into a future model as our experiments suggest limits for specific parameters. It is of interest to note here that, although we have shown a degree of correlation, or 'coupling', of K^+-ATPase activity to K^+ and anion permeation, and an uncoupling of these functions when H^+ permeability is increased, we have not experimentally observed a classical tight coupling between the driving force and the H^+ gradient. That is, assuming ATP provides the energy for proton transport we would expect the system to achieve equilibrium when the energetic driving force equals the electrochemical potential gradient of H^+ across the vesicles. As the system approaches equilibrium conditions, ATP hydrolysis would be diminished for the 'well-coupled', non-leaky system. Significant H^+ leak pathways provide the basis for the steady state conditions of the pump-leak model.

Gastric oxyntic cells secrete a fluid with a pH of about 0.8, thus these cells produce the largest proton gradient in biological system, being greater than 10^6 fold. Under the conditions that obtain within the cell this would mean that only one, certainly no more than two, H^+ could be secreted/ATP utilized [41]. If the K^+-ATPase studied here was the primary gastric proton pump, we would not expect the system to approach conditions of equilibrium and a slowing, or reversal, of ATP utilization until the intravesicular pH decreased significantly below pH 1. The lowest intravesicular pH we have recorded with fluorescent amine probes was 2.5, or a 10^4 fold H^+ gradient with an external pH of 6.5 [14]. It would thus appear that proton leaks, either as free H^+ or as the protonated form of the probe itself, are operating to prevent maximum gradient formation and/or the approach to conditions of equilibrium where net ATP hydrolysis would be slowed. These specialized conditions of the gastric ATPase may also be the reason why we have been unsuccessful thus far in using proton gradients (up to 4 pH units) to drive net synthesis of ATP (unpublished results).

Appendix

In this section, a computer simulation model for ion transport in gastric vesicles will be presented. The model consists of active and passive pathways

for ion movements. The active pathway is a H^+/K^+ exchange pump which transports n_H^K potassium ions out of the vesicle for each H^+ ion transported in. The passive pathways will be described by the permeability coefficient for each ion. This model is not intended to be a quantitative summary of experimental data, but rather should be treated as a general description of the system. Emphasis will be placed on the pattern of behavior of the system with respect to changes in parameters. Part of the derivations presented here follow the treatment described by Macey [42].

The following symbols are used: P_H, P_K, P_{Cl}, permeability of H^+, K^+, Cl^-, respectively (in cm $\cdot$ min^{-1}); J_H, J_K, J_{Cl}, net flux of H^+, K^+, Cl^- across the membrane. The sign convention used is positive into, and negative out of, the vesicle (in mol $\cdot$ cm^{-2} $\cdot$ min^{-1}); $[H]_i$, $[K]_i$, $[Cl]_i$, concentration of H^+, K^+ and Cl^- in the internal vesicular space (in mol $\cdot$ l^{-1}); $[H]_0$, $[K]_0$, $[Cl]_0$, concentration of H^+, K^+ and Cl^- in the external medium (assumed to be constant); V_i, vesicular volume/mg of protein (in l $\cdot$ mg^{-1}); r, radius of the vesicle (in cm); ψ, membrane potential (in mV); F, R and T have their usual significance.

The net flux of H^+ can be expressed as the sum of passive diffusional flux, J_H^{diff}, and flux due to active transport, J_H^{pump}.

$$J_H = J_H^{diff} + J_H^{pump} \tag{1}$$

J_H^{diff} is given by the following equation:

$$J_H^{diff} = \frac{F\Psi/RT}{e^{F\Psi/RT} - 1} P_H\{[H]_0 - [H]_i\, e^{F\psi/RT}\} \tag{2}$$

which is the result of direct integration of the Nernst-Planck equation with the constant field assumption (also assumed that ionic activities can be replaced by concentrations). To model the active flux, J_H^{pump}, we will assume that the rate of the pump can be described by simple Michaelis-Menten kinetics with internal K^+ as substrate, and for each turnover of the pump N_{ATP}^H mol of H^+ are transported.

$$J_H^{pump} = \frac{r}{3}\frac{N_{ATP}^H}{V_i}\frac{V_{max}[K]_i}{K_M + [K]_i} \tag{3}$$

where V_{max} is the maximum rate of the pump (expressed as mol $\cdot$ mg^{-1} $\cdot$ min^{-1}) and K_m is the concentration of K^+ at half-maximal pump rate.

The total flux J_H is related to $[H]_i$ by the following equation:

$$J_H = \frac{r}{3}\frac{d}{dt}[H]_i \tag{4}$$

Substitute Eqns. 2—4 into 1, and assume $N_{ATP}^H = 1$, we have:

$$\frac{d}{dt}[H]_i = \frac{3}{r}\frac{F\Psi/RT}{e^{F\Psi/RT} - 1} P_H\{[H]_0 - [H]_i\, e^{F\Psi/RT}\} + \frac{1}{V_i}\frac{V_{max}[K]_i}{K_M + [K]_i} \tag{5}$$

Similar equation can be obtained for K^+ and Cl^-:

$$\frac{d}{dt}[K]_i = \frac{3}{r}\frac{F\Psi/RT}{e^{F\Psi/RT} - 1} P_K\{[K]_0 - [K]_i\, e^{F\Psi/RT}\} - \frac{n_K^H}{V_i}\frac{V_{max}[K]_i}{K_M + [K]_i} \tag{6}$$

$$\frac{d}{dt}[Cl]_i = \frac{3}{r}\frac{F\Psi/RT}{e^{F\Psi/RT}-1} P_{Cl}\{[Cl]_0 e^{F\Psi/RT} - [Cl]_i\}$$

In Eqn. 6, the following expression for the active flux of K^+ through the pump was used:

$$J_K^{pump} = -n_H^K J_H^{pump} \tag{8}$$

In Eqn. 7, it was assumed that no active transport of Cl^- occurred in these vesicles. The net active current, J_i^{pump}, is given by the sum of active H^+ and K^+ currents. Using Eqn. 8, it can be written as:

$$J_i^{pump} = J_K^{pump} + J_H^{pump} = (1 - n_H^K) J_H^{pump} \tag{9}$$

Condition for macroscopic electrical neutrality gives

$$J_i^{pump} + J_H + J_K - J_{Cl} = 0 \tag{10}$$

Substituting the individual expression for J_H, J_K, J_{Cl} and J_i^{pump} into Eqn. 10 and rearranging, the membrane potential can be expressed as:

$$\Psi = \frac{RT}{F} \ln \frac{P_K[K]_0 + P_H[H]_0 + P_{Cl}[Cl]_i - \frac{RT}{F\Psi}(1 - n_H^K) J_H^{pump}}{P_K[K]_i + P_H[H]_i + P_{Cl}[Cl]_0 - \frac{RT}{F\Psi}(1 - n_H^K) J_H^{pump}} \tag{11}$$

In the case of an electroneutral exchange pump for H^+ and K^+; then $n_H^K = 1$, and the ψ is then given by

$$\Psi = \frac{RT}{F} \ln \frac{P_K[K]_0 + P_H[H]_0 + P_{Cl}[Cl]_i}{P_K[K]_i + P_H[H]_i + P_{Cl}[Cl]_0} \tag{12}$$

Eqns. 5—7 and 12 were solved numerically using an interactive simulation language written by Auslander [43]. All calculations were performed using a PDP-11 mini-computer.

Acknowledgements

We gratefully acknowledge the participation of Marcia Berman in the early phases of the work on the various anion effects, and the skillful technical assistance of Jean Poulter. This work was supported in part by a grant from the U.S. Public Health Service, AM 10141.

References

1 Forte, J.G., Ganser, A.L. and Tanisawa, A. (1974) Ann. N.Y. Acad. Sci. 242, 245—267
2 Chang, H., Saccomani, G., Rabon, E., Schackmann, R. and Sachs, G. (1977) Biochim. Biophys. Acta 464, 313—327
3 Ganser, A.L. and Forte, J.G. (1973) Biochim. Biophys. Acta 307, 169—180
4 Lee, J., Simpson, G. and Scholes, P. (1974) Biochem. Biophys. Res.Commun. 60, 825—852
5 Sachs, G., Chang, H.H., Rabon, E., Schackmann, R., Lewin, M. and Saccomani, G. (1976) J. Biol. Chem. 251, 7690—7698

6 Schackmann, R., Schwartz, A., Saccomani, G. and Sachs, G.J. (1977) Membrane Biol. 32, 361—381
7 Heinz, E. and Durbin, R.P. (1959) Biochim. Biophys. Acta 31, 246—247
8 Forte, J.G., Adams, P.H. and Davies, R.E. (1963) Nature 197, 874—876
9 Durbin, R.P. (1964) J. Gen. Physiol. 4, 735—748
10 Forte, J.G. (1969) Am. J. Physiol. 216, 167—174
11 Forte, J.G. and Machen, T.E. (1975) J. Physiol. 244, 33—51
12 Kasbekar, D.K. and Durbin, R.P. (1965) Biochim. Biophys. Acta 105, 472—482
13 Sachs, G., Shah, G., Strych, A., Cline, G. and Hirschowitz, B.I. (1972) Biochim. Biophys. Acta 266, 625—638
14 Lee, H.C. and Forte, J.G. (1978) Biochim. Biophys. Acta 508, 339—356
15 Lee, H.C., Quintanilha, A.T. and Forte, J.G. (1976) Biochem. Biophys. Res. Commun. 72, 1179—1186
16 Forte, J.G., Ganser, A.L., Beesley, R. and Forte, T.M. (1975) Gastroenterology 69, 175—189
17 Sanui, H. (1974) Anal. Biochem. 60, 489—504
18 Eibl, H. and Lands, W.E.M. (1969) Anal. Biochem. 30, 51—57
19 Ellman, G.L. (1959) Arch. Biochem. Biophys. 82, 70—77
20 Boyne, A.L. and Ellman, G.L. (1972) Anal. Biochem. 46, 639—653
21 Murphy, A.J. (1976) Biochem. 15, 4492—4496
22 Udenfriend, S., Stein, S., Bohlen, R., Dairman, W., Leingouber, W. and Weigle, M. (1972) Science 178, 871—872
23 Lowry, O.L., Rosebrough, N.J., Farr, A.L. and Randall, R.J. (1951) J. Biol. Chem. 193, 265—275
24 Branton, D. (1966) Proc. Natl. Acad. Sci. U.S. 55, 1048—1056
25 Deamer, D.W. and Baskin, R.J. (1969) J. Cell Biol. 42, 296—307
26 Inesi, G. and Seales, D. (1974) Biochemistry 13, 3298—3306
27 Boland, R., Martonosi, A. and Tillack, T.W. (1974) J. Biol. Chem. 249, 612—623
28 Forte, J.G., Ganser, A.L. and Ray, T.K. (1976) in Gastric Hydrogen Ion Secretion (Kasbekar, D.K., Sachs, G. and Rehm, W., eds.), pp. 302—330, Marcel Dekker, New York
29 Overath, P. and Trauble, H. (1973) Biochemistry 12, 2625—2634
30 Herketh, T.R., Smith, G.A., Houslay, M.D., McGill, K.A., Birdsall, N.J.M., Metcalfe, J.G. and Warren, G.B. (1976) Biochemistry 15, 4145—4151
31 Grisham, C.M. and Barnett, R.E. (1973) Biochemistry 13, 2635—2637
32 Ray, T.K. and Forte, J.G. (1976) Biochim. Biophys. Acta 443, 451—467
33 Forte, T.M. and Forte, J.G. (1971) J. Ultrastruct. Res. 37, 322—334
34 Limlomwongse, L. and Forte, J.G. (1970) Am. J. Physiol. 219, 1717
35 Pressman, B.C. and Hanes, D.H. (1969) in Molecular Basis of Membrane Function (Tosteson, D.C., ed.), pp. 221—246, Prentice-Hall, Englewood Cliffs, NJ
36 Pinkerton, M., Steinrauf, L.K. and Dawkins, P. (1969) Biochem. Biophys. Res. Commun. 35, 512—518
37 Ashton, R. and Steinrauf, L.K. (1970) J. Membrane Biol. 49, 547—556
38 Blok, M.C., De Gier, J. and Van Deenen, L.L.M. (1974) Biochim. Biophys. Acta 367, 210—224
39 Stark, G., Ketterer, B., Bent, R. and Lauger, P. (1971) Biophys. J. 11, 981—994
40 Hogben, C.A.M. (1962) Circulation 26, 1179—1188
41 Machen, T.E. and Forte, J.G. (1979) Transport across Biological Membranes (Giebisch, G., ed.), Vol. 4, Springer Verlay, Heidelberg, in the press
42 Macey, R.I. (1978) Physiology of Membrane Disorders (Andreoli, T.E., Hoffman, J.F. and Fanestil, D., eds.), pp. 125—146, Plenum, NY
43 Auslander, D.M. (1974) J. Dyn. Syst. Meas. Control Trans. ASME (Ser. G, No. 3) 96, 261